JOURNAL OF SOLID STATE CHEMISTRY **85**, 262–269 (1990)

The Preparation and Properties of Cobalt-Doped II–VI Chalcogenides

C-M. NIU, R. KERSHAW, K. DWIGHT, AND A. WOLD

Department of Chemistry, Brown University,
Providence, Rhode Island 02912

Received September 13, 1989; in revised form December 4, 1989

Samples of cobalt-doped ZnS, ZnSe, CdS, and CdSe were prepared by the direct combination of the elements. The limit of solubility of cobalt in these systems was established. Magnetic measurements indicate that the antiferromagnetic interactions of the cobalt in the zinc systems were greater than those observed in the cadmium chalcogenides. Single crystals of cobalt-doped zinc chalcogenides were grown by chemical vapor transport. Their IR transmission was measured and the cobalt concentration for maximum hardness was determined.

Introduction

The II–VI compounds ZnS, ZnSe, CdS, and CdSe have been studied extensively since they offer a variety of unique device applications. Compounds containing transition metal ions, e.g., $Zn_{1-x}Mn_xSe$, $Zn_{1-x}Co_xSe$, and $Cd_{1-x}Fe_xSe$, are known as dilute magnetic semiconductors. The presence of magnetic ions leads to a number of unusual electronic and optical properties which are due to the interaction of the magnetic ion with band electrons as well as to the exchange interaction between the magnetic ions themselves (*1–3*). Magnetic semiconductors containing manganese have been extensively studied and their magnetic properties, including the ion–ion exchange interaction, are well understood (*1–3*). Several studies have been carried out on iron-based dilute magnetic semiconductors (*4–7*). More recently, attention has focused on Co-containing systems (*8*). The Co(II)($3d^7$) has an orbital singlet ground state in a tetrahedral coordination environment and it is anticipated to be easily introduced into II–VI compounds. Becker and Lutz (*9*) have reported on the solubility of CoS (i.e., Co(II)) in ZnS and CdS. Its solubility in ZnS increases with temperature within the range from 500 to 1000°C. At 1000°C the solubility is 41 mol% in ZnS, but only 20 mol% in CdS. The substitution of zinc and cadmium by cobalt causes a regular decrease in the unit cell constants of ZnS. The solubility of CoS (i.e., Co(II)) in ZnS determined by Hall (*10*) is 33 mol% at 850°C; however, there is no report about the solubility of CoSe in ZnSe and CdSe.

The optical properties of Co(II) in II–VI compounds have been studied rather extensively in samples containing cobalt impurities (*11*). The infrared luminescence spectra due to the $^4T_2$–$^4A_2$ electronic transition as well as the ESR spectra for cobalt ions as impurities in several wide-gap II–VI compounds have been reported (*12–14*). Furthermore, ZnS is used as an IR window material because of its wide transmission range in the infrared. However, both ZnS

0022-4596/90 $3.00

and ZnSe are soft, which limits their suitability for some applications as IR windows. In our previous studies of the systems $Zn_{1-x}Ni_xS$ and $(ZnSe)_{1-x}(GaP)_x$ (*15, 16*) it was noted that the IR spectra of $Zn_{1-x}Ni_xS$ and $(ZnSe)_{1-x}(GaP)_x$ are not changed appreciably from those of pure ZnS and ZnSe, but the hardness is enhanced significantly.

Ni(II)($3d^8$) prefers an octahedral coordination, and it has been shown that it is difficult to introduce a significant quantity of Ni(II) into the ZnS structure (*17*). However, as reported, up to 41 at.% of cobalt can be substituted for zinc at 1000°C. Thus it should be possible to modify the properties of II–VI compounds using cobalt as a component. This study concerns itself with the preparation and characterization of the systems Co–ZnS(Se) for both powder and single crystal samples and Co–CdS(Se) for powder samples. Attention is focused on such problems as the solubility limits, the magnetic behavior of Co(II) in a tetrahedral site, as well as IR transmission, hardness and stability of the materials.

Experimental

Preparation of Polycrystalline Samples

Polycrystalline samples with different compositions were prepared by using stoichiometric amounts of zinc metal (Gallard and Schlesinger 99.9995%), cadmium (Cominco EM 8001 99.999%), sulfur (Gallard and Schlesinger 99.999%), selenium (UMC 23333 99.999%), and cobalt (prereduced in Ar/H_2 (85/15)). The reactants (total weight approximately 3 g) for $Zn_{1-x}Co_xS$ and $Zn_{1-x}Co_xSe$ were sealed in evacuated 12 mm i.d. × 60 mm silica tubes and heated in the following manner: 450°C for 24 hr, 500°C for 24 hr, 600°C for 12 hr, 700°C for 12 hr, 800°C for 12 hr, 900°C for 24 hr, and 950°C for 72 hr. The samples were ground under a nitrogen atmosphere prior to the 950°C heating, after heating for 24 hr at 950°C, and after 48 hr at 950°C. For $Cd_{1-x}Co_xS$ and $Cd_{1-x}Co_xSe$, the highest temperature reached was 750°C. The samples were ground prior to the 750°C treatment, after heating for 24 hr at 750°C, and after 48 hr at 750°C. Finally, the samples were cooled in the furnace to room temperature before removal.

In order to confirm that the distribution of Co(II) in the samples is independent of the preparative methods, the same compositions of $Zn_{1-x}Co_xS$ were also prepared by codecomposition of a mixture of the sulfates under an atmosphere of H_2S. Stoichiometric amounts of zinc and cobalt metal were added to sufficient 1 : 1 sulfuric acid to give a 20% excess of H_2SO_4 over the stoichiometry of $Zn_{1-x}Co_xSO_4$ in order to promote reaction of all the cobalt. After being dried on a hot plate, the $Zn_{1-x}Co_xSO_4$ was placed in a silica boat and heated in a flow of $H_2S/Ar(2/1)$ in the following manner: 250°C for 6 hr, 500°C for 6 hr, and 700°C for 6 hr. The samples were ground prior to the 700°C heating. Finally, samples were sealed in evacuated 12-mm silica tubes and heated at 950°C for 24 hr.

Crystal Growth

Single crystals of $Zn_{1-x}Co_xS$ and $Zn_{1-x}Co_xSe$ have been grown by chemical vapor transport using iodine as the transport agent. Polycrystalline samples were placed in a silica tube (14 mm o.d. × 12 mm i.d.) which had been previously heated to near the melting point in order to minimize any nucleation sites. The tube was evacuated to 10^{-5} Torr and freshly sublimed iodine was introduced as the transport agent at a concentration of 5 mg/ml. The tube was sealed off and enclosed in a tightly wound Kanthal coil (to even out temperature gradients) and the whole assembly was placed in a three-zone furnace. The crystal growth temperature program consisted of setting the furnace to back transport mode for one day, equilibrating the furnace to the maximum temperature for 3 hr, and finally, cooling the growth zone at 1°C/hr to the growth temperature. Optimum crystal growth for $Zn_{1-x}Co_xS$ occurred when the charge zone was maintained at 900°C and the growth zone at 875°C and optimum crystal growth for $Zn_{1-x}Co_xSe$ occurred when the charge zone was maintained at 850°C and the growth zone at 825°C. The transport process was carried out for 2 weeks for $Zn_{1-x}Co_xS$ and for 1 week for $Zn_{1-x}Co_xSe$, and the typical crystal size was 8 × 5 × 5 mm. The actual composition of each single crystal was determined from magnetic susceptibility measurements.

Characterization

X-ray powder diffraction patterns of the samples were obtained using a Philips diffractometer and monochromated high intensity $CuK\alpha_1$ radiation ($\lambda = 1.5405$ Å). For qualitative phase identification, diffraction patterns were taken over the range $12° < 2\theta < 72°$ with a scan rate of 1° 2θ/min, while cell parameters were determined from scans taken at 0.25° 2θ/min. Precise lattice parameters were obtained from these reflections using a least-squares refinement program which corrects for the systematic errors of the diffractometer.

Optical measurements on polished single crystal slices were performed at room temperature on a Perkin-Elmer 580 single beam scanning infrared spectrophotometer. The measurements were performed in the transmission mode over the range 2.5–50 μm. Transmission through the sample was normalized to the signal obtained in the absence of the sample.

The microhardness measurements (Knoop indenter) were made on crystals using a Kentron microhardness tester. The results were obtained using a diamond indenter with 25-g loads for $Zn_{1-x}Co_xS$ and 10 g for $Zn_{1-x}Co_xSe$.

The stability of these compounds toward oxidation was determined by grinding a small crystal and heating the resulting powder in flowing oxygen (60 ml/min) and monitoring the change in weight during the heating period. The decomposition temperature was determined as the temperature where the weight of the sample began to change.

Magnetic susceptibilities were measured from liquid nitrogen temperature to 573 K using a Faraday balance at a field strength of 10.4 kOe. Honda–Owens (field dependency) plots were also made and all magnetic susceptibility data were corrected for diamagnetism.

Results and Discussion

Polycrystalline samples of $Zn_{1-x}Co_xS$, $Zn_{1-x}Co_xSe$, $Cd_{1-x}Co_xS$, and $Cd_{1-x}Co_xSe$ were prepared directly from the elements. X-ray diffraction patterns indicated that the products were single phase and could be indexed on the basis of a cubic unit cell (*18*) for $Zn_{1-x}Co_xS$ and $Zn_{1-x}Co_xSe$ and a hexagonal unit cell for $Cd_{1-x}Co_xS$ and $Cd_{1-x}Co_xSe$. The samples with different amounts of cobalt were subjected to X-ray analysis in order to obtain the cell parameters (Tables I–III). The cell volumes are plotted as functions of cobalt concentration for $Zn_{1-x}Co_xS$ and $Zn_{1-x}Co_xSe$ in Fig. 1 and for $Cd_{1-x}Co_xS$ in Fig. 2. At cobalt concen-

TABLE I

PROPERTIES OF POLYCRYSTALLINE $Zn_{1-x}Co_xS$

Compound	Cell parameter a (Å)	μ (BM)	Weiss constant (K)
ZnS	5.409(2)	—	—
$Zn_{.98}Co_{.02}S$	5.407(2)	4.17	−15
$Zn_{.94}Co_{.06}S$	5.406(2)	4.42	−109
$Zn_{.90}Co_{.10}S$	5.403(2)	4.59	−198
$Zn_{.86}Co_{.14}S$	5.401(2)	—	—
$Zn_{.82}Co_{.18}S$	5.398(2)	4.92	−403
$Zn_{.78}Co_{.22}S$	5.395(2)		
$Zn_{.74}Co_{.26}S$	5.392(2)		
$Zn_{.70}Co_{.30}S$	5.389(2)		
$Zn_{.66}Co_{.34}S$	5.386(2)		

TABLE II

PROPERTIES OF POLYCRYSTALLINE $Zn_{1-x}Co_xSe$

Compound	Cell parameter a (Å)	μ (BM)	Weiss constant (K)
ZnSe	5.668(2)	—	—
$Zn_{.98}Co_{.02}Se$	5.670(2)	4.22	−15
$Zn_{.94}Co_{.06}Se$	5.667(2)	4.52	−115
$Zn_{.90}Co_{.10}Se$	5.663(2)	4.74	−229
$Zn_{.86}Co_{.14}Se$	5.661(2)		
$Zn_{.82}Co_{.18}Se$	5.659(2)		

trations less than 36.4 at.% for $Zn_{1-x}Co_xS$ and 18.6 at.% for $Zn_{1-x}Co_xSe$, the cell volumes decrease linearly with increasing amounts of cobalt. This indicates that the smaller Co(II) could be substituted for the larger Zn(II) as desired. The cell volumes do not change for samples of $Zn_{1-x}Co_xS$ containing 38 and 42 at.% cobalt. Similarly, the $Zn_{1-x}Co_xSe$ samples with 22 and 26 at.% cobalt do not change within experimental error (±0.002 Å in their a parameter). Thus the data shown in Fig. 1 indicate that the solubility limit of cobalt in polycrystalline ZnS is 36.4 at.% at 950°C. This is in agreement with the results reported by Becker and Lutz (*9*). The solubility limit of Co(II) in polycrystalline ZnSe is 18.6 at.% at 950°C. The solubility of Co(II) in CdS was determined to be 14 at.% as shown in Fig. 2, and 6 at.% in CdSe. Comparing the limit of substitution by Co(II) in the four compounds, it can be seen that increasing the size of both cations and anions decreases the limit of substitution. The cell parameters listed in Tables I–III indicate that the cell volumes of Co–CdS(Se) decrease more significantly than those of Co–ZnS(Se). This is consistent with the relative sizes of these ions in tetrahedral sites, namely: 0.60 Å for Zn(II), 0.78 Å for Cd(II), and 0.58 Å for Co(II) (*19*).

The magnetic susceptibilities of polycrystalline samples given in Figs. 3 and 4 were measured in order to determine the cobalt concentration in the single crystals which were grown. The effective moments and Weiss constants which were obtained for the polycrystalline standards of known compositions (prepared in sealed tubes) were reproducible, bracketed the values obtained for single crystals, and served to uniquely characterize the cobalt content. Samples of $Zn_{1-x}Co_xS$ prepared by direct reaction of the elements as well as the codecomposition of the sulfates give the same moment and Weiss constant for the same composition. This indicates that the distribution of cobalt in the samples is independent of the methods of preparation. The

TABLE III

PROPERTIES OF POLYCRYSTALLINE $Cd_{1-x}Co_xS$ AND $Cd_{1-x}Co_xSe$

Compound	Cell parameter (Å) a	c	μ (BM)	Weiss constant (K)
CdS	4.137(2)	6.716(2)	—	—
$Cd_{.98}Co_{.02}S$	4.130(2)	6.706(2)	4.00	−17
$Cd_{.94}Co_{.06}S$	4.119(2)	6.690(2)	4.04	−50
$Cd_{.90}Co_{.10}S$	4.108(2)	6.672(2)	4.11	−101
$Cd_{.86}Co_{.14}S$	4.096(2)	6.657(2)	4.13	−145
CdSe	4.302(2)	7.014(2)	—	—
$Cd_{.98}Co_{.02}Se$	4.296(2)	7.003(2)	4.07	−12
$Cd_{.94}Co_{.06}Se$	4.279(2)	6.979(2)	4.18	−49

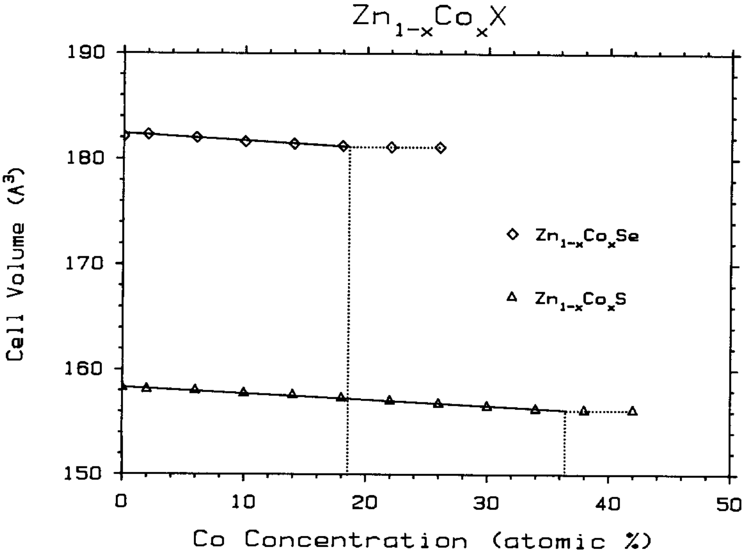

FIG. 1. Variation of cell volume with cobalt concentration in $Zn_{1-x}Co_xS$ and $Zn_{1-x}Co_xSe$.

measured moments and Weiss constants, as determined from their high temperature susceptibilities, are given in Tables I–III for the four systems. The magnetic moments and negative Weiss constants increase with increasing cobalt content for all systems, and the antiferromagnetic interactions in the zinc systems are stronger than those in the cadmium systems. This can be related to the fact that superexchange interactions

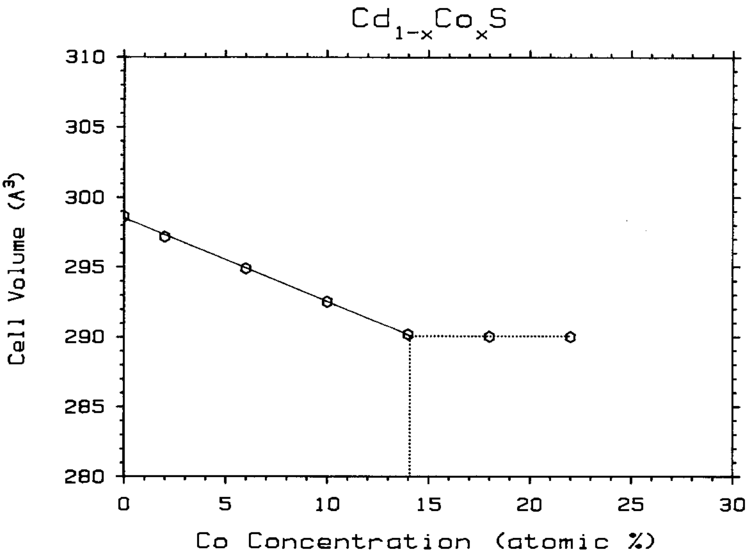

FIG. 2. Variation of cell volume with cobalt concentration in $Cd_{1-x}Co_xS$.

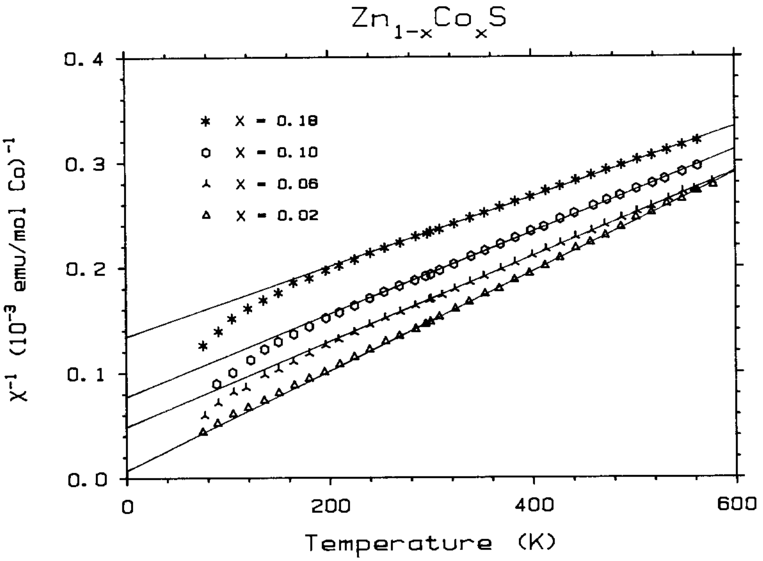

FIG. 3. Inverse magnetic susceptibility as a function of temperature for members of the system $Zn_{1-x}Co_xS$.

between adjacent cobalt ions via chalcogen ions are further apart in the cadmium systems.

The above results are consistent with the behavior reported for Co(II) in tetrahedral coordination (*20, 21*). In this coordination, the Co(II) $^4T_{9/2}$ free ion level is split by the tetrahedral crystal field into an upper $^4T_1$ orbital triplet, a $^4T_2$ triplet, and a lower $^4A_2$ orbital singlet ground state (*22*). The Co(II)

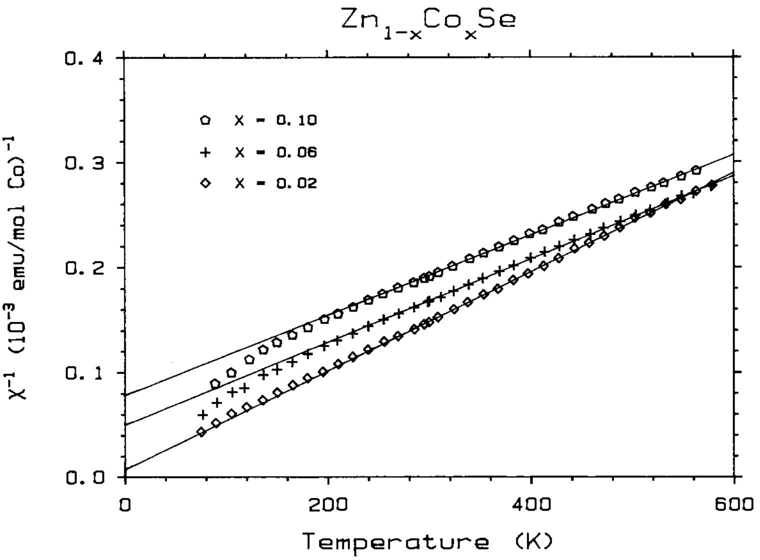

FIG. 4. Inverse magnetic susceptibility as a function of temperature for members of the system $Zn_{1-x}Co_xSe$.

TABLE IV

PROPERTIES OF $Zn_{1-x}Co_xS$ SINGLE CRYSTALS

Compound	Knoop hardness (kg/mm²)	IR window (μm)	Stability limit (°C)
ZnS	160	2.5–14	530
$Zn_{.99}Co_{.01}S$	210	3.8–14	510
$Zn_{.95}Co_{.05}S$	240	3.8–14	490
$Zn_{.89}Co_{.11}S$	240	3.8–14	470
$Zn_{.84}Co_{.16}S$	173	3.8–14	455

ground state has a significant orbital angular momentum component due to spin–orbit mixing with the low-lying $^4T_4$ triplet, producing an effective Lande *g* factor of 2.27 (*23*), and giving rise to a greater than spin-only moment. The negative Weiss constant at low cobalt concentrations can be attributed to distant neighbor Co–Co antiferromagnetic interactions. The rapid increase of this negative value with increasing cobalt concentration can be related to the presence of much stronger nearest neighbor interactions.

Single crystals of $Zn_{1-x}Co_xS$ and $Zn_{1-x}Co_xSe$ were grown by chemical vapor transport using iodine as the transport agent. The color of single crystals changes from colorless in pure ZnS to green, becoming darker with increasing cobalt content for $Zn_{1-x}Co_xS$. In the system $Zn_{1-x}Co_xSe$, the color changes from light yellow for ZnSe to deep yellow with increasing cobalt content. The concentration of cobalt in the crystals was determined from their magnetic susceptibility measurements by comparison with polycrystalline standards of known cobalt composition. The maximum cobalt substitution obtained under the experimental conditions described above is 16 at.% in ZnS and 4 at.% in ZnSe. The properties of the crystals are summarized in Tables IV and V.

The IR transmission data summarized in Tables IV and V indicate that pure ZnS crystals transmit in the range of 2.5 to 20 μm. Crystals containing cobalt give the same IR transmission at the long wavelength end, but appear to cut off at about 4.0 μm with no observable change with increasing cobalt concentration. Probably the cutoff results from tetrahedral cobalt *d–d* transitions (*12–14*).

The hardness (Knoop hardness number of the crystals containing cobalt shows a significant increase compared to the pure end member. There is an increase to a maximum value and then a decrease with increasing cobalt content for $Zn_{1-x}Co_xS$. The measured hardness of pure ZnS is 160 kg/mm² and that of ZnSe is 101 kg/mm², and samples of $Zn_{.95}Co_{.05}S$ and $Zn_{.96}Co_{.04}Se$ gave hardness values of 240 and 167 kg/mm². From Tables IV and V, it can also be seen that the introduction of cobalt into ZnS and ZnSe decreases their stability toward oxidation in flowing oxygen. The onset temperature of decomposition, which is considered as the point where there is an observable weight loss (.01 mg), decreases continually with increasing cobalt content. Pure ZnS and ZnSe start to decompose in flowing oxygen 530 and 420°C, respectively. The samples of $Zn_{.95}Co_{.05}S$ and $Zn_{.98}Co_{.02}Se$ began to decompose at 490 and 410°C, respectively.

Conclusions

The solubility of cobalt in ZnS was determined to be 36.4 at.% at 950°C, and 14 at.% in CdS at 750°C. In this paper, the solubility of cobalt, rather than that of cobalt sulfide as given by previous investigators is re-

TABLE V

PROPERTIES OF $Zn_{1-x}Co_xSe$ SINGLE CRYSTALS

Compound	Knoop hardness (kg/mm²)	IR window (μm)	Stability limit (°C)
ZnSe	101	2.5–20	420
$Zn_{.995}Co_{.005}Se$	110	4.0–20	415
$Zn_{.98}Co_{.02}Se$	120	4.0–20	410
$Zn_{.96}Co_{.04}Se$	167	4.0–20	403

ported, because it is cobalt(II) which is being substituted for zinc in the various II–VI phases. This is in agreement with the results reported by Becker and Lutz (*9*). The solubility of cobalt was found to be 18.6 at.% in ZnSe at 950°C, and 6 at.% in CdSe at 750°C. It was shown that increasing the size from Zn(II) to Cd(II) or S^{2-} to Se^{2-} decreases the solubility limit. Magnetic measurements show similar paramagnetic behavior with antiferromagnetic interactions which increase with increasing cobalt concentrations in all four systems. The antiferromagnetic interactions in zinc systems are stronger than those in cadmium systems. This can be attributed to differences in the cobalt–cobalt distances observed in the compounds. Crystals containing cobalt show a cutoff at the short wavelength end of their IR spectra, but give the same IR transmission as that of pure ZnS and ZnSe at the long wavelengths. Substitution of cobalt significantly increases the hardness of both ZnS and ZnSe. However, the stability of the samples toward oxidation in a flowing oxygen atmosphere decreases slightly with cobalt concentration.

Acknowledgments

This research was partially supported by NSF DMR-890-1270, the Office of Naval Research, the Exxon Education Foundation, and Eastman Kodak Company.

References

1. N. B. Brandt and V. V. Moshchalkov, *Adv. Phys.* **33,** 193 (1984).
2. J. K. Furdyna, *J. Appl. Phys.* **53,** 7637 (1982).
3. J. K. Furdyna and N. Samarth, *J. Appl. Phys.* **61,** 3526 (1987).
4. A. V. Komarov, S. M. Ryabchenko, and O. V. Terletskii, *Phys. Status Solidi B* **102,** 603 (1980).
5. A. Twardowski, P. Gold, W. J. M. de Jonge and M. Demianiuk, *Solid State Commun.* **64,** 63 (1987).
6. A. Petrou, X. Liu, G. Waytena, J. Warnock, and W. Giriat, *Solid State Commun.* **61,** 767 (1987).
7. D. Heiman, A. Petrou, E. D. Isaacs, S. H. Bloom, Y. Shapira, and W. Giriat, *Phys. Rev. Lett.* **60,** 1876 (1988).
8. B. T. Jonker, J. J. Kerbs, and G. A. Prinz, *Appl. Phys. Lett.* **53,** 450 (1988).
9. W. Becker and H. D. Lutz, *Mater. Res. Bull.* **13,** 907 (1978).
10. W. E. Hall, U.S. Geol. Survey Prof. Paper, 424-B, 271 (1961).
11. S. M. Uba and J. M. Baraowski, *Phys. Rev. B* **17,** 69 (1978).
12. P. Koidt and A. Rauber, *J. Phys. Chem. Solids* **35,** 1061 (1974).
13. A. P. Radlinski, *Phys. Status Solidi* **86,** 41 (1978).
14. A. P. Radlinski, *J. Lumin.* **18–19,** 147 (1979).
15. P. Wu, R. Kershaw, K. Dwight, and A. Wold, *Mater. Res. Bull.* **24,** 49 (1989).
16. H-S. Shen, G-Q. Yao, X-C. He, K. Dwight, and A. Wold, *Mater. Res. Bull.* **23,** 153 (1988).
17. G. K. Czamanske and F. E. Goff, *Econ. Geol.* **68,** 256 (1973).
18. Powder Diffraction File compiled by the JCPDS International Centre for Diffraction Data, Card Nos. 5-566, 5-522, 6-134, and 8-459.
19. R. D. Shannon and P. S. Gumerman, "Table of Effective Ionic Radii," duPont de Nemours & Co., Wilmington, DE.
20. E. Agostinelli, L. Gastaldi, and S. Viticoli, *J. Phys. Chem. Solids* **12,** 1345 (1985).
21. D. Fiorani and S. Viticoli, *J. Solid State Chem.* **26,** 101 (1978).
22. A. Abragam and B. Bleaney, "Electron Paramagnetic Reasonance of Transition Ions," p. 470, Oxford Univ. Press, London, 1970.
23. U. Kaufman and J. Schneider, *Solid State Commun.* **25,** 1113 (1978).